

## Microenvironment-Driven Modulation of A2E Photoreactivity and Fluorescence Under Blue Light

Deepak Basyal, Shiva Kumar Bhandari, and Hye Jin Kim\*

*College of Pharmacy, Keimyung University, Daegu, 42601, Republic of Korea*

**Abstract** – A2E, a major pyridinium bisretinoid component of retinal lipofuscin, functions as a photosensitizer that undergoes blue light-induced oxidation, contributing to oxidative stress in age-related macular degeneration (AMD). This study investigated whether lipophilic antioxidants and non-antioxidant hydrophobic molecules protect A2E primarily through reactive oxygen species (ROS) quenching, modulation of its local microenvironment, or both. A2E was irradiated with blue light in the presence or absence of hydrophobic additives: palmitic acid (PA), vitamin E,  $\beta$ -carotene, lutein, zeaxanthin, and zeaxanthin dipalmitate (ZDP). Fluorescence spectroscopy assessed photophysical changes. A2E degradation was quantified using reverse-phase LC-MS with optimized electrospray ionization, distinguishing actual A2E loss from fluorescence artifacts. All additives significantly reduced A2E degradation, with protection strongly correlated with hydrophobicity. ZDP preserved about 76% of A2E, and even non-antioxidant PA offered marked protection. Fluorescence spectra showed compound-specific emissions and, notably, increased A2E fluorescence intensity with a blue shift, particularly with ZDP and PA, suggesting enhanced co-localization in lipid-rich domains. These results reveal two complementary protective mechanisms: classical ROS scavenging by carotenoids and vitamin E, and microenvironment remodeling by highly lipophilic molecules like ZDP and PA. The microenvironmental remodeling effects of lipophilic compounds remain speculative and warrants further investigation. Thus, strategies targeting both ROS neutralization and A2E's hydrophobic niche may effectively mitigate blue-light-driven retinal damage in AMD.

**Keywords** – A2E, AMD, Photooxidation, Bisretinoid, Carotenoid

### Introduction

Retinal autofluorescence arises mainly from lipofuscin in retinal pigment epithelium (RPE), and bisretinoids fluorophores isolated from these cells show matching spectral properties, indicating they are the primary source of fundus autofluorescence.<sup>1</sup> The fluorescence properties of lipofuscin granules can serve as an indicator to detect early degenerative changes in the retina and RPE.<sup>2</sup> A2E (Fig. 1A) is a predominant pyridinium bisretinoid generated as a byproduct of the vision cycle and sequestered within the lysosomes of RPE cells after phagocytosis of rod outer segments.<sup>3</sup> Structurally, A2E contains a central pyridinium ring (Fig. 1A) that carries a permanent positive charge and two polyene side chains derived from retinal. These extended conjugated polyene chains confer strong visible-light absorbance and are responsible for the

characteristic photoreactivity of A2E.<sup>4</sup> Moreover, its amphiphilic structure promotes accumulation in RPE lysosomes and contributes to lipofuscin formation.<sup>3</sup> Recent studies show that A2E biosynthesis and photophysics may drive RPE cell death, linking A2E accumulation to AMD-induced central vision loss in the adult population.<sup>4,5</sup> Similar to other photosensitizers, A2E contains conjugated polyene arms with delocalized  $\pi$  electrons, that facilitate efficient energy and electron transfer and lower its oxidation potential.<sup>6,7</sup> Importantly, A2E is not merely a biomarker of aging; it is a chemically active chromophore that absorbs blue light and converts it into oxidative stress through reactive oxygen species (ROS) production, including singlet oxygen.<sup>8</sup> Crucially, however, A2E photoreactivity is not an immutable molecular property; it is tightly regulated by the local environment. Since A2E's excited state is strongly environment-dependent, its emission maximum, intensity, and quantum yield are influenced by local polarity and packing.<sup>9</sup> Polar environment stabilizes the excited state, producing a red shift and reduced fluorescence intensity via enhanced non-radiative relaxation, whereas a hydro-

\*Author for correspondence

Hye Jin Kim, Ph.D., College of Pharmacy, Keimyung University, Daegu, 42601, Republic of Korea  
Tel: +82-54-580-6649; E-mail: [hjk0901@kmu.ac.kr](mailto:hjk0901@kmu.ac.kr)

phobic environment limits solvent-mediated quenching and often increases emission.<sup>7,10</sup>

A study reports that A2E is depleted more extensively upon light exposure in less polar conditions, at a lower concentration of anionic surfactant, and in gel-phase rather than fluid-ordered phospholipid liposomes<sup>7</sup>. Moreover, A2E aggregation incurs photooxidation/photodegradation, while A2E redistribution between biphasic phases enables fluorescence recovery after photobleaching.<sup>7,11</sup> As a lipid-retinoid conjugate embedded within the hydrophobic core of lysosomal lipofuscin granules, A2E experiences a lipid matrix that directly shapes its photophysical and photochemical behavior.<sup>12</sup>

Blue light-driven oxidation of the bisretinoid A2E is implicated in retinal oxidative stress and AMD, yet the relative contributions of direct antioxidant scavenging versus microenvironmental control remain a key unresolved question. We investigated how selected hydrophobic compounds (Fig. 1C) modulate the fluorescence and photochemical stability of A2E in a simplified *in vitro* model system (5% DMSO in water) following controlled blue-light irradiation. Our primary objective was whether these agents affect A2E integrity directly through antioxidant or excited state quenching activity, suppressing photochemical reactions, or indirectly by reshaping the local microenvironment of A2E, thereby changing its fluorescence quantum yield without necessarily altering A2E abundance. To achieve this, we employed two orthogonal analytical approaches—fluorescence spectroscopy and liquid chromatography-mass spectrometry (LC-MS)—allowing independent assessment of photophysical changes and definitive quantification of chemical degradation. By correlating these orthogonal measures, we were able to discriminate between genuine molecular loss and changes in emission efficiency driven by environmental or compound-mediated effects. This study helps in elucidating the precise mechanistic role of these hydrophobic agents in modulating A2E phototoxicity.

## Experimental

**General experimental procedures** – Fluorescence measurements of A2E with the indicated compound were performed on a SpectraMax iD3 microplate reader (Molecular Devices Inc, Sunnyvale, CA) using 96-well flat-bottom black plates (SPL Life Sciences). Blue-light irradiation (430 nm) was carried out using a blue-light irradiator (Miraestc, Korea). Quantification was conducted using 2D LC/triple quadrupole MS (NFEC-2025-02-303305) (Model G11958-65638; Agilent Technologies,

Santa Clara, CA, USA), and data acquisition and processing were performed using Agilent Mass Hunter workstation software. Zeaxanthin and zeaxanthin dipalmitate (ZDP) were previously isolated in our laboratory from *Lycium chinensis* fruits (goji berries). Palmitic acid (PA), vitamin E, lutein, and  $\beta$ -carotene were purchased from Sigma-Aldrich. Stock solutions (1 mM) of all compounds were prepared in DMSO (Sigma-Aldrich) and stored under nitrogen at  $-80^{\circ}\text{C}$ . All experiments were conducted under dim red-light conditions in a dark environment to minimize photoisomerization and photodegradation of the compounds.

**Synthesis of A2E** – A2E was synthesized according to a previously published method<sup>13</sup> and purified using a 1290 Infinity II Preparative HPLC System (NFEC-2025-01-302570). HPLC, mass spectrometry, and UV-visible characteristics confirmed the identity and purity of A2E. Stock solution of A2E (2.5 mM) was prepared in DMSO and stored under nitrogen at  $-80^{\circ}\text{C}$ .

**Blue-Light-Induced Photooxidation of A2E: Fluorescence Analysis** – PA, vitamin E,  $\beta$ -carotene, lutein, zeaxanthin, and ZDP were evaluated for their effects on A2E photoprotection under blue-light irradiation by monitoring changes in fluorescence intensity. A2E (25  $\mu\text{M}$ ) was mixed with an equimolar concentration of each compound in 5% DMSO (v/v) in water. Fluorescence intensity was measured for 50  $\mu\text{L}$  aliquots before and after 3 min of blue-light irradiation. Fluorescence spectra were acquired at room temperature as relative fluorescence units from 480 to 800 nm (10 nm increments), using 6 nm bandpass slits and 430 nm excitation

**Blue-Light-Induced Photooxidation of A2E** – HPLC chromatograms were acquired for 25  $\mu\text{M}$  A2E immediately before and after irradiation with 430 nm blue light to monitor photooxidative degradation. HPLC analysis was conducted using an Agilent 1260 Infinity II system equipped with OpenLab CDS (Agilent Technologies, Santa Clara, CA, USA). Atlantis T3 C18 column (100  $\times$  2.1 mm, 3  $\mu\text{m}$ , 100  $\text{\AA}$ ; Waters, Milford, MA, USA) at  $40^{\circ}\text{C}$  with a flow rate of 0.4 mL/min and a 10  $\mu\text{L}$  injection volume was used for analysis. Elution was performed using a gradient of solvent A (0.1% trifluoroacetic acid, TFA, in water) and solvent B (acetonitrile, containing 0.1% TFA), with detection at 430 nm. The gradient was programmed as follows: 0–5 min, 30% B; 5–8 min, 30–75% B, 8–12 min, 75–100% B, 12–30 min, 100% B. The column was then equilibrated to initial conditions with a 5-minute post-run.

**Blue-Light-Induced Photooxidation of A2E: LC-MS Analysis** – A2E remaining after irradiation was quantified

by LC-MS by monitoring changes in the chromatographic peak area of intact A2E. Briefly, A2E samples were incubated in the absence or presence of the indicated study compounds and then exposed to blue-light irradiation at room temperature. After irradiation, samples were analyzed by LC-MS, and intact A2E was identified by its characteristic retention time and  $m/z$ . The A2E signal was quantified by integrating the A2E extracted-ion chromatogram (EIC) peak area, and photodegradation was expressed as the percentage change in A2E peak area after irradiation. For each condition, the A2E remaining was calculated by normalizing the post-irradiation A2E peak area to the corresponding non-irradiated control. A2E quantification was carried out on an Agilent 2D-LC/MS platform. Chromatographic separation was achieved on an Agilent EclipsePlus C18 column ( $2.1 \times 50$  mm,  $1.8 \mu\text{m}$ ) using methanol (B) and water (A) containing 0.1% formic acid as the mobile phase. The gradient was as follows: 90% B (0–0.5 min), 90–100% B (0.5–1.5 min), 100% B (1.5–5.0 min), and re-equilibration at 90% B (5.0–7.0 min). The flow rate and column temperature were 0.3 mL/min and  $40^\circ\text{C}$ , respectively.  $5 \mu\text{L}$  was injected per run, and UV/Visible detection was monitored at 430 nm. Quantification by tandem mass spectrometry was performed in MRM mode by monitoring the transition at  $m/z$   $592.4 \rightarrow 418.5$  to determine the peak area of A2E. Mass spectrometric settings were optimized

for A2E analysis using a positive mode electrospray ionization (ESI) source. The fragmentation voltage and collision-induced dissociation (CID) energy were optimized to be 200 V and 44 eV, respectively. The sheath gas was set to 11 L/min at  $350^\circ\text{C}$ , the nebulizer pressure to 40 psi, and the drying gas to 7 L/min with a dry gas temperature of  $350^\circ\text{C}$ . Capillary and nozzle voltage were maintained at 5000 V and 500 V, respectively, to ensure efficient ionization and stable A2E signal intensity.

**Statistical analysis** – Data were analyzed using GraphPad Prism (v8.02; GraphPad Software, San Diego, CA, USA). Results are presented as mean  $\pm$  SEM from at least three independent experiments ( $n = 3$ ). The ability of the study compounds to prevent blue-light-induced A2E photooxidation was assessed by one-way ANOVA followed by Tukey's post hoc test.

## Results and Discussion

The spectral and fluorescence transformation is the hallmark of photooxidative modulation of the A2E chromophore. The oxidative cleavage of the extended conjugated polyene arms of A2E (Fig. 1A) results in the formation of smaller, less conjugated species and highly reactive carbonyl compounds. These photofragments contribute to the pathogenic cascade in the RPE cells, which is central to atrophic age-related macular degeneration

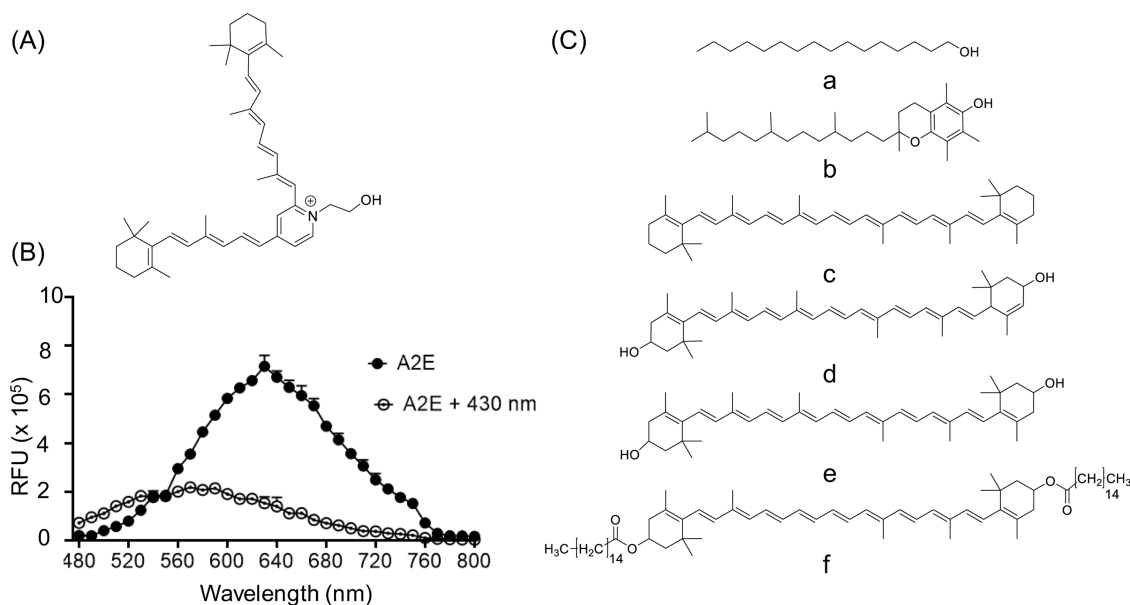


**Fig. 1.** (A) Chemical structure of A2E. (B) Representative fluorescence emission spectrum of 25  $\mu\text{M}$  A2E recorded upon excitation at 430 nm in 5% (v/v) DMSO in water, showing the characteristic emission profile across 480–800 nm. Fluorescence (relative fluorescence units, RFU) was recorded at an excitation of 430 nm. (C) Chemical structures of hydrophobic compounds examined in this study, selected to represent carotenoids, lipid-soluble antioxidants, and non-antioxidant fatty acids: a: palmitic acid, b: vitamin E, c:  $\beta$ -carotene, d: lutein, e: zeaxanthin, f: zeaxanthin dipalmitate.

(AMD).<sup>14</sup>

Our central hypothesis was whether destructive photo-oxidation of A2E could be intercepted by modulating the immediate chemical environment of A2E with protective, hydrophobic molecules (Fig. 1C). The rationale is that such compounds could co-localize with the amphiphilic A2E and shield it via photophysical and/or chemical mechanisms. We demonstrated that co-incubation of A2E with compounds such as PA, vitamin E,  $\beta$ -carotene, lutein, zeaxanthin, and ZDP significantly preserved A2E molecules from blue light-induced degradation compared to the irradiated control (Fig. 4).

Fluorescence spectroscopy revealed that native A2E emits a broad band peak spanning 480–800 nm, with its peak near 625–630 nm (Fig. 1B). After exposure to 430 nm blue light, the overall fluorescence intensity dropped sharply, and the peak exhibited a blue shift. This significant loss in intensity aligns with photobleaching caused by photooxidative changes or breakdown of the polyene chromophore, which lowers its ability to emit light. The blue shift suggests that irradiation not only reduces the amount of intact A2E but also alters the fluorescent properties, possibly through the formation of oxidized or less conjugated photoproducts. A similar decrease in A2E fluorescence, accompanied by a blue-shifted emission maximum after blue-light irradiation, has also been reported in a previous study.<sup>7</sup> Taken together, these findings highlight A2E's high sensitivity to short-wavelength light and show that both reduced fluorescence and a shift in emission peak can monitor its photochemical changes.

Fig. 2 shows fluorescence emission spectra for A2E and all selected hydrophobic additives across 480–800 nm, with maxima clustered around 590–630 nm. Relative

to A2E alone, adding hydrophobic compounds increases fluorescence intensity and, in several cases, shifts the apparent emission maximum to shorter wavelengths (i.e., a blue shift). In fluorescence control experiments, none of the hydrophobic additives showed detectable fluorescence under the acquisition conditions used for A2E. Therefore, the fluorescence signal observed in A2E-additive mixtures is not attributable to intrinsic fluorescence from the additives under 430 nm excitation.

HPLC chromatograms of 25  $\mu$ M A2E recorded before and after 430 nm blue-light irradiation reveal pronounced photooxidative degradation of A2E with the concomitant emergence of multiple photoproduct peaks (Fig. 3). The results of the present study are consistent with previous reports that blue light preferentially induces degradation

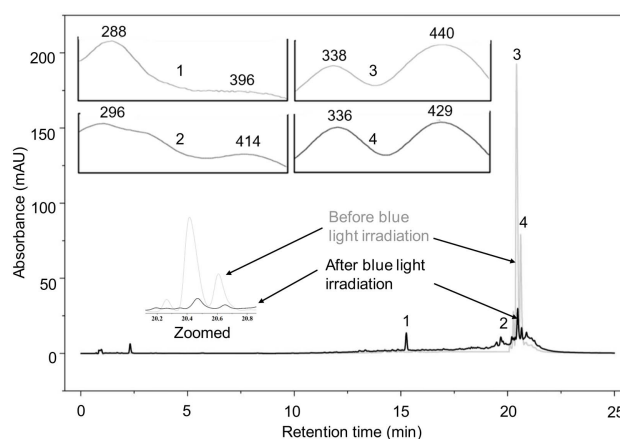


**Fig. 3.** HPLC monitoring of 25  $\mu$ M A2E at 430 nm before and after exposure to blue light demonstrates loss of the parent A2E and isoA2E peaks (3, 4) and formation of photooxidized species (1, 2), consistent with blue-light-induced photooxidation at 430 nm. Insets show the UV-visible absorbance spectra, with  $\lambda$  max (nm) indicated for the corresponding chromatographic peaks.

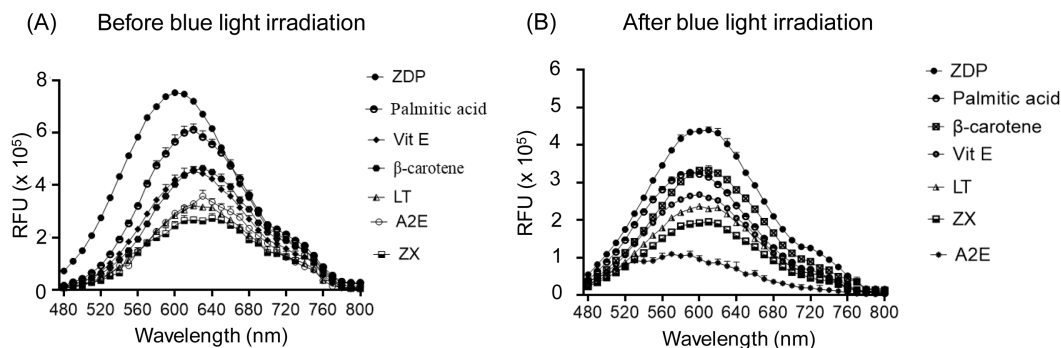


**Fig. 2.** Fluorescence emission spectra of A2E in the absence or presence of equimolar hydrophobic compounds before and after blue-light irradiation. Fluorescence (relative fluorescence units, RFU) was recorded at an excitation of 430 nm and A2E concentration of 25  $\mu$ M. (A) Emission spectra recorded before irradiation, showing compound-dependent modulation of A2E fluorescence intensity and spectral profile. (B) Emission spectra recorded after blue-light exposure (430 nm, 3 mins), showing an overall reduction in fluorescence intensity following irradiation. Fluorescence spectra are presented as relative fluorescence unit (RFU) versus emission wavelength (nm). ZX: zeaxanthin, LT: lutein, Vit E: vitamin E, ZDP: zeaxanthin dipalmitate.

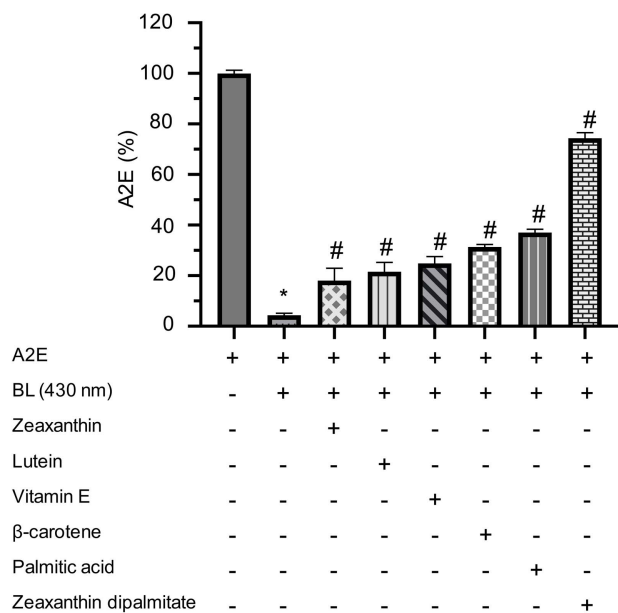


**Fig. 4.** A2E remaining after blue light irradiation, quantified by LC-MS. Data are expressed as mean  $\pm$  SEM ( $n = 3$ ). Statistical significance was determined by one-way ANOVA followed by Tukey's post hoc test. Bars labeled with special characters indicate statistically significant differences ( $p < 0.0001$ ). \* $p$ , significantly different from unirradiated A2E control; # $p$ , significantly different from irradiated A2E control (A2E + BL).

of A2E.<sup>15,16</sup>

Blue light exposure triggered a rapid and pronounced decline in A2E levels in LC-MS analysis. After 3 min exposure, the A2E + BL group showed a drastic reduction in A2E levels, retaining only about 5% of its initial concentration (Fig. 4). These results demonstrate that even brief blue-light exposure induces extensive A2E photooxidation. However, when hydrophobic compounds were introduced, they significantly reduced this loss, as confirmed by statistical comparison with the A2E + BL control. Notably, ZDP offered the most robust protection, preserving A2E up to 76% of the initial condition. Lutein and vitamin E also provided considerable stabilization, while  $\beta$ -carotene and PA showed more modest, but still significant protection effects compared to the A2E + BL condition. Collectively, these findings highlight that A2E photooxidation is highly dependent on its hydrophobic surroundings and can be markedly suppressed by lipid-soluble compounds.

Zeaxanthin, lutein,<sup>17</sup> and  $\beta$ -carotene<sup>18</sup> are effective quenchers of singlet oxygen ( $^1O_2$ ), the primary reactive oxygen species generated by A2E acting as a photosensitizer. By rapidly dissipating the energy from  $^1O_2$ , these carotenoids can break the photooxidative chain reaction before it damages A2E. Similarly, vitamin E, a

chain-breaking antioxidant, can neutralize peroxy radicals, offering a complementary pathway within a lipid phase.<sup>19</sup> Our results align with this literature, confirming their direct protective role against A2E photodegradation. The greater inhibition of A2E photooxidation by ZDP relative to zeaxanthin is plausibly explained less by intrinsic radical scavenging chemistry and more by micro-environmental partitioning and retention. The profound protection from ZDP highlights a critical concept. ZDP, a C16 ester of zeaxanthin, possesses high lipophilicity compared to the parent carotenoid.<sup>20</sup> This would favor its stable partitioning into hydrophobic domains where A2E resides, potentially creating a highly concentrated protective shield that is more effective than free zeaxanthin. PA, while lacking a canonical antioxidant functional group, may exert its protective effect by altering the physical properties of the local environment. It could increase molecular packing and microviscosity, thereby sterically hindering oxygen diffusion to the photoexcited A2E and reducing the efficiency of the oxidative reaction.<sup>9,21</sup> It also favors A2E partitioning into less photoreactive assemblies and limits A2E conformational freedom relevant to reactive excited-state pathways. Because PA lacks singlet oxygen-quenching or radical-scavenging activity, its protective effect possibly supports a microenvironment-mediated mechanism rather than chemical antioxidant activity. This kind of indirect photoprotection due to altered lipid architecture, rather than direct ROS scavenging, has precedent in oxidative stress models, in which membrane composition controls the photooxidation rate and spatial confinement. The potential role of non-antioxidative lipophilic compounds through micro-environmental remodeling remains hypothetical and is not directly supported by experimental evidence in the present study. This mechanism is presented as a speculative possibility that requires further investigation. Our data extend this concept to A2E, suggesting that even non-antioxidant hydrophobes can reduce A2E oxidation by reshaping the local environment where A2E absorbs blue light and reacts with oxygen.

Our finding demonstrates that this photodegradation is not an immutable process but is highly susceptible to modulation by the local hydrophobic environment. This microenvironment-driven modulation of A2E photo-reactivity highlights that chemical stability is governed not only by intrinsic antioxidant activity but also by lipid-mediated co-localization and spatial confinement. While classical antioxidants like carotenoids and vitamin E provide protection, the superior performance of zeaxanthin dipalmitate suggests that the lipophilicity and stable co-

localization of a protective agent with A2E is an exceptional strategy for preventing its phototoxicity. Importantly, fluorescence enhancement alone did not necessarily correlate with the preservation of intact A2E, underscoring the necessity of LC-MS-based quantification to distinguish genuine chemical protection from photo-physical artifacts. These results provide a strong mechanistic basis for the use of targeted lipophilic antioxidants in therapeutic strategies aimed at mitigating retinal photo-degenerative diseases like AMD.

### Acknowledgements

This work was supported by the National Research Foundation of Korea (NRF) grant funded by the Korea government (MSIT) (No. RS-2024-00344799), and by the Korea Basic Science Institute (National Research Facilities and Equipment Center) grant funded by the Korea government (MSIT) (No. RS-2024-00402577).

### Conflict of Interest

The authors declare that they have no conflicts of interest.

### References

- (1) Ben-Shabat, S.; Parish, C. A.; Hashimoto, M.; Liu, J.; Nakanishi, K.; Sparrow, J. R. *Bioorg. Med. Chem. Lett.* **2001**, *11*, 1533–1540.
- (2) Feldman, T. B.; Dontsov, A. E.; Yakovleva, M. A.; Ostrovsky, M. A. *Biophys. Rev.* **2022**, *14*, 1051–1065.
- (3) Sparrow, J. R.; Fishkin, N.; Zhou, J.; Cai, B.; Jang, Y. P.; Krane, S.; Itagaki, Y.; Nakanishi, K. *Vision Res.* **2003**, *43*, 2983–2990.
- (4) Fisher, C. R.; Ferrington, D. A. *Invest. Ophthalmol. Vis. Sci.* **2018**, *59*, AMD41-AMD47.
- (5) Andreev, V.; Yakovleva, M.; Kostyukov, A.; Sokolova, V.; Shcheslavskiy, V.; Goltsman, G.; Feldman, T.; Kuzmin, V.; Ostrovsky, M.; Morozov, P. *J. Biophotonics.* **2025**, *19*, e202500418.
- (6) Kim, S. R.; Jockusch, S.; Itagaki, Y.; Turro, N. J.; Sparrow, J. R. *Exp. Eye Res.* **2008**, *86*, 975–982.
- (7) Liu, Z.; Ueda, K.; Kim, H. J.; Sparrow, J. R. *PLoS One* **2015**, *10*, e0138081.
- (8) Kanofsky, J. R.; Sima, P. D.; Richter, C. *Photochem. Photobiol.* **2003**, *77*, 235–242.
- (9) Ragauskaitė, L.; Heckathorn, R. C.; Gaillard, E. R. *Photochem. Photobiol.* **2001**, *74*, 483–488.
- (10) Kim, H. J.; Sparrow, J. R. *J. Lipid Res.* **2018**, *59*, 1620–1629.
- (11) Yamamoto, K.; Zhou, J.; Hunter, J. J.; Williams, D. R.; Sparrow, J. R. *Invest. Ophthalmol. Vis. Sci.* **2012**, *53*, 3536–3544.
- (12) Sparrow, J. R.; Boulton, M. *Exp. Eye Res.* **2005**, *80*, 595–606.
- (13) Sparrow, J. R.; Parish, C. A.; Hashimoto, M.; Nakanishi, K. *Invest. Ophthalmol. Vis. Sci.* **1999**, *40*, 2988–2995.
- (14) Wang, Z.; Keller, L. M.; Dillon, J.; Gaillard, E. R. *Photochem. Photobiol.* **2006**, *82*, 1251–1257.
- (15) Sparrow, J. R.; Zhou, J.; Ben-Shabat, S.; Vollmer, H.; Itagaki, Y.; Nakanishi, K. *Invest. Ophthalmol. Vis. Sci.* **2002**, *43*, 1222–1227.
- (16) Dillon, J.; Wang, Z.; Avalle, L. B.; Gaillard, E. R. *Exp. Eye Res.* **2004**, *79*, 537–542.
- (17) Kim, S. R.; Nakanishi, K.; Itagaki, Y.; Sparrow, J. R. *Exp. Eye Res.* **2006**, *82*, 828–839.
- (18) Cantrell, A.; McGarvey, D. J.; Truscott, T. G.; Rancan, F.; Böhm, F. *Arch. Biochem. Biophys.* **2003**, *412*, 47–54.
- (19) Yamauchi, R. *Food Sci. Technol. Int.* **1997**, *3*, 301–309.
- (20) Kan, X.; Yan, Y.; Ran, L.; Lu, L.; Mi, J.; Zhang, Z.; Li, X.; Zeng, X.; Cao, Y. *Food Hydrocoll.* **2020**, *105*, 105781.
- (21) Furso, J.; Zadlo, A.; Szweczyk, G.; Sama, T. J. *Cell Biochem. Biophys.* **2020**, *78*, 415–427.

Received January 19, 2026

Revised March 11, 2026

Accepted March 12, 2026